

Journal of Mechanics of Materials and Structures

B-SPLINES COLLOCATION EIGENANALYSIS OF 2D ACOUSTIC PROBLEMS

Christopher G. Provatidis

Volume 9, No. 3

May 2014



B-SPLINES COLLOCATION EIGENANALYSIS OF 2D ACOUSTIC PROBLEMS

CHRISTOPHER G. PROVATIDIS

We continue our research on the performance of CAD-based global approximation to the analysis of 2D acoustic problems. In addition to previous “boundary-only” Coons and transfinite Gordon–Coons interpolations, we now investigate the quality of the solution when utilizing “tensor product B-splines” interpolation. For the latter, we propose a global collocation method that is successfully compared with the well known Galerkin–Ritz formulation. Particular attention is paid to the handling of Neumann boundary conditions as well as to the role of multiplicity of internal knots. The theory is supported by two numerical examples, one for a rectangular and the other for a circular acoustic cavity in which the approximate solution rapidly converges towards the exact solution.

1. Introduction

The tendency in contemporary computer methods in applied mechanics and engineering is to integrate solid modeling (computer-aided-design or CAD) with analysis (computer-aided-engineering or CAE) using NURBS interpolation, in such a way that both the geometry and the mechanical variables (displacement, temperature, etc.) are mathematically expressed in a similar manner (global approximation) [Cottrell et al. 2009]. In fact, though the nonuniform B-splines (NURBS) of today is, chronologically speaking, the fifth important formulation applied to the mathematical description of CAD models, the same integration can be achieved with using any of the previous formulations. The first bivariate formula was proposed in 1964–1967 by Coons [1967], the second by Gordon [1971] and the third in 1966–1971 by Bézier [1971]. Furthermore, B-splines are chronologically the fourth formula in CAD practice. Although older mathematical formulations of splines were first published by Schoenberg [1946], they became very popular only after 1972 when de Boor [1972] proposed his computationally efficient algorithms. Finally, B-splines were later modified on the basis of weighting coefficients, thus producing the popular NURBS of today, which are fully controlled sculptured surfaces [Piegl 1991; Piegl and Tiller 1995]. For a detailed review we refer to [Farin et al. 2002].

Concerning mechanical analysis in problems of solids and structures including acoustics, it is well known that there are three main methodologies: the popular finite element method (FEM), the boundary element method (BEM), and the promising global collocation method ([Provatidis 2008b; 2009b; Provatidis and Ioannou 2010] and about 300 references therein). For the sake of brevity, finite volume, finite difference, mesh-less and mesh-free methodologies are not commented on. So far, FEM [Höllig 2003] and BEM [Cabral et al. 1990; 1991] have been applied in conjunction with tensor product B-splines in several engineering problems. Also, Coons–Gordon transfinite interpolation has been extensively used in conjunction with the Galerkin–Ritz formulation; for an overview we refer to [Provatidis 2012] and

Keywords: B-splines, Galerkin–Ritz, global collocation, eigenvalues, CAD/CAE.

literature therein. Our conclusion in that article is that rapid CAD-based global collocation methods have to be applied instead of time-consuming domain Galerkin–Ritz methods.

For the first time, in 2005 the author expressed the above general idea of implementing a *global collocation* scheme in conjunction with CAD-based approximation [Provatidis 2006, p. 6704], while he continued with numerical applications in potential problems under Dirichlet [Provatidis 2008b] and Neumann [Provatidis 2009b] boundary conditions, as well as in plane stress elastostatics [Provatidis and Ioannou 2010]. Concerning eigenvalue and time response structural analysis, in 2008 he published a couple of papers [Provatidis 2008a; 2008c] (1D problems), and also he supervised a thesis concerning 2D acoustics and 2D elastodynamics in conjunction with Lagrange polynomials [Filippatos 2010]. It is worth mentioning that isogeometric collocation methods were recently presented by others [Auricchio et al. 2010].

It is well known that B-splines collocation methods were initially developed by mathematicians, well before engineers understood that CAD-based Galerkin–Ritz methods require high computing effort, a fact that motivated them to investigate their replacement by isogeometric collocation schemes [Hughes et al. 2010]. For a detailed review of 273 papers covering the period 1934–1989 we refer to [Fairweather and Meade 1989], whereas recent works are cited in a survey [Bialecki et al. 2011]. A fair comparison between B-spline collocation and Galerkin methods on the basis of the same bandwidth (and not the same degree of shape functions) in one spatial dimension is [Kwok et al. 2001]. However, most works are limited to one-dimensional problems [de Boor 2001, Chapter XV], where, for cubic B-splines, the key point is to use two collocation points between any two breakpoints, thus resulting in as many equations as the number of unknowns; this is strictly related to using double knots (de Boor, personal communication, 2007). On the other hand, excellent results have been obtained in some particular examples using for collocation the images of either Greville or Demko abscissae [Auricchio et al. 2010].

It is remarkable that de Boor’s software, aiming at the solution of one-dimensional (1D) elliptic nonlinear problems, although incorporated in Matlab (Spline Toolkit) long ago, is not still applicable to the solution of eigenvalue and time-marching problems “as is”. As confirmed by the absence of relevant publications, the need of a computational environment to solve 2D and 3D problems is of great engineering interest.

Within this context, this paper reports on the performance of the B-splines-based global collocation method for the eigenvalue analysis of two-dimensional acoustic cavities under arbitrary, Dirichlet or Neumann boundary conditions. Particular attention is paid to the treatment of the free-free problem in order to bypass the singularities that sometimes may appear at the four corner points of the reference square. Moreover, the role of the multiplicity of internal knots is thoroughly investigated, and particularly the performance of the proposed least-squares scheme in conjunction with single knots is studied. The theory is sustained by two numerical examples, one for a rectangular and the other for a circular acoustic cavity, in which the proposed collocation method is successfully compared with its competitive Galerkin–Ritz scheme, using either tensor product B-splines or/and conventional finite elements, for the same mesh density.

2. B-splines as a global 2D functional set

2.1. General. Let us consider a rectangular domain $\Omega = (ABCD) = [0, a] \times [0, b]$ in \mathbb{R}^2 . The axis origin is chosen at the corner A , whereas the Cartesian axes x and y lie on the sides AB and AD , respectively.

Sides AB and CD are uniformly divided into n_x segments, while BC and DA are uniformly divided into n_y segments. This leads to $n_x + 1$ breakpoints along AB and CD , and $n_y + 1$ breakpoints along BC and DA . Although it is possible to use different degrees for the spline polynomials in the x - and y -directions, we will use a single degree $p_x = p_y = p$, with $p \geq 3$, since we are dealing with a second order PDE (acoustics). As a result, the univariate function $u(x, 0)$ along the side AB can be interpolated via a piecewise polynomial B-spline of p -th degree in x , and the function $u(0, y)$ along the side DA via a piecewise polynomial B-spline of p -th degree in y .

2.2. One-dimensional shape functions. This section refers to either the x - or y -directions (along the sides AB and DA , respectively). Below, n corresponds to either subdivision n_x or n_y , whereas the domain $[0, L]$ corresponds to either of the intervals $[0, a]$ or $[0, b]$.

Let us assume a given number of n subdivisions of the interval $[0, L]$, with breakpoints x_0, \dots, x_n , and a given polynomial degree p . In its original form [Schoenberg 1946; Schoenberg and Whitney 1953], the B-splines formula includes a complete polynomial of p -th degree for the entire domain $[0, a]$, plus $(n - 1)$ truncated monomials $\langle x - x_i \rangle_+^p$, $i = 1, \dots, n$. In this way, the total number of coefficients becomes $(n + p)$, and we refer to a multiplicity of internal knots equal to one, which ensures C^{p-1} -continuity. Therefore, in the particular case of a cubic approximation ($p = 3$), the total number of coefficients becomes $(n + 3)$, which ensures C^2 -continuity.

In contrast, if we alternatively consider the above complete polynomial of p -th degree for the entire domain $[0, L]$ plus the aforementioned $(n - 1)$ truncated monomials $\langle x - x_i \rangle_+^p$, and additionally $(n - 1)$ truncated monomials $\langle x - x_i \rangle_+^{p-1}$, $i = 1, \dots, n$, the total number of coefficients becomes $(2n + p - 1)$, and then we refer to internal multiplicity equal to two, which ensures C^{p-2} -continuity; for example, C^1 -continuity and $2(n + 1)$ coefficients, when $p = 3$.

In the modern approach [Piegl and Tiller 1995; de Boor 2001], these coefficients are associated with what's called *control points*. In more detail, we start with the above-mentioned breakpoints

$$\{\mathbf{x}_b\} = [x_0, \dots, x_n], \tag{1}$$

and then we introduce the *knot vector* $\{\mathbf{V}\}$,

$$\{\mathbf{V}\} = [v_0, \dots, v_m], \tag{2}$$

which highly depends on the chosen *multiplicity* λ of internal knots (usually single or double):

- multiplicity $\lambda = 1$: $\{\mathbf{V}\}_{\lambda=1} = [\underbrace{x_0, \dots, x_0}_{p+1}, x_1, x_2, \dots, x_{n-1}, \underbrace{x_n, \dots, x_n}_{p+1}]$, (3)

- multiplicity $\lambda = 2$: $\{\mathbf{V}\}_{\lambda=2} = [\underbrace{x_0, \dots, x_0}_{p+1}, \underbrace{x_1, x_1}_2, \underbrace{x_2, x_2}_2, \dots, \underbrace{x_{n-1}, x_{n-1}}_2, \underbrace{x_n, \dots, x_n}_{p+1}]$. (4)

Therefore, Equations (3) and (4) lead to the unified relationship

$$m = 2(p + 1) + \lambda(n - 1) - 1, \quad \lambda = 1, 2. \tag{5}$$

Based on the above-mentioned computed knot vector $\{\mathbf{V}\}$, the vector of control points is denoted by

$$\{\mathbf{P}\} = [\mathbf{P}_0, \dots, \mathbf{P}_{n_c}], \tag{6}$$

where the number of control points ($n_c + 1$) is related to the number of elements in the knot vector ($m + 1$) as

$$m = n_c + p + 1. \quad (7)$$

Then, for every position $x \in [0, L]$, with normalized coordinate $\xi = x/L \in [0, 1]$, we can determine the values of $n_c + 1$ basis functions, $N_{i,p}(x)$ or $N_{i,p}(\xi)$, $i = 0, \dots, n_c$:

(1) The Cartesian coordinate is approximated as

$$x(\xi) = \sum_{i=0}^n N_i(\xi) \cdot x_i. \quad (8)$$

(2) The variable is approximated as

$$u(\xi) = \sum_{i=0}^n N_i(\xi) \cdot a_i. \quad (9)$$

It is worth mentioning that the coefficients a_i in (9) are generally different from the nodal values u_i associated to the breakpoints, except at the ends where $a_0 = u_0$ and $a_n = u_n$.

Remark. In the particular case in which there are no internal breakpoints (i.e., $n = 1$), (5) implies that the knot vector consists of $m + 1 = 2(p + 1)$ elements, whence (7) implies that the number of control points becomes $n_c = p$. In other words, in case of Bézier (Bernstein polynomial) representation, the number of coefficients is identical with those involved in a Taylor series, that is, a full polynomial of degree p .

2.3. Two-dimensional global shape functions. Given the uniform subdivisions n_x and n_y of the intervals $[0, a]$ and $[0, b]$, respectively, the breakpoints along each of the four sides (AB , BC , CD , and DA) are determined. Moreover, given the multiplicity of internal knots, as well as the polynomial degrees p_x and p_y , the control points in the x - and y -direction are also determined. If the patch is curvilinear, then x - and y -coordinates have to be replaced by the ξ - and η -normalized coordinates, respectively.

While in the older B-splines formulation [Schoenberg 1946; Schoenberg and Whitney 1953] the degrees of freedom are associated to the $(n_x + 1) \times (n_y + 1)$ nodal points x_{ij} lying at the intersections of i -th and j -th lines perpendicular to the axes and passing through the *breakpoints* (x_i, y_j) , in this “modern” formulation we have to deal only with the tensor product of q *control points*. Therefore, in the case of cubic approximation ($p_x = p_y = p = 3$), we distinguish two cases. In the first case, the multiplicity of internal knots is $\lambda = 1$, so the tensor product consists of $q = (n_x + 3) \times (n_y + 3)$ coefficients a_{ij} . In the second case, the multiplicity of internal knots is $\lambda = 2$, so the tensor product consists of $q = 4(n_x + 1)(n_y + 1)$ coefficients a_{ij} .

Therefore, according to the selected value of multiplicity λ (1 or 2), the two-dimensional global shape functions are given by

$$\lambda = 1: \quad \phi_{ij}(x, y) = N_i(x) \cdot N_j(y), \quad i = 0, \dots, (n_x + 3) \wedge j = 0, \dots, (n_y + 3), \quad (10)$$

$$\lambda = 2: \quad \phi_{ij}(x, y) = N_i(x) \cdot N_j(y), \quad i = 0, \dots, 2(n_x + 1) \wedge j = 0, \dots, 2(n_y + 1) \quad (11)$$

(the double subscript is to emphasize the two directions).

The continuity of the approximation is prescribed by both the polynomial degree and the multiplicity. For cubic splines, if the multiplicity is one, then the univariate approximation is C^2 -continuous (whereas for 2D, $u \in C^{2,2}(\Omega_{\text{st}})$). In contrast, if the multiplicity is two, then the univariate approximation is C^1 -continuous (whereas for 2D, $u \in C^{1,1}(\Omega_{\text{st}})$); $\Omega_{\text{st}} = [0, 1] \times [0, 1]$ is the *standard* reference square.

In the general case of higher polynomial degrees, $p > 3$, the B-splines approximation ensures $C^{p-\lambda}$ -continuity when the multiplicity of inner knots is λ ($1 \leq \lambda \leq p - 1$). The most usual case for the numerical solution of an ordinary differential equation by collocation is to require C^1 -continuity (multiplicity $\lambda = p - 1$) and take λ collocation points between any two successive breakpoints. Under these circumstances, after encountering the two boundary conditions we obtain as many equations as the number of unknowns (this observation is useful to static problems, for which the reader is referred to Appendix A, and dynamic ones). Therefore, the minimum value of multiplicity λ is 1 (C^{p-1} -continuity), whereas the maximum one is $p - 1$ (C^1 -continuity).

In general, the q control points are divided into two categories, that is, $n_{c,\text{in}}$ in the interior of the domain Ω and $n_{c,b}$ near the boundary ($q = n_{c,\text{in}} + n_{c,b}$). In more detail, if a side of the quadrilateral $ABCD$ (e.g., AB) is straight, the corresponding control points lie on this side (AB). In contrast, if the side is curved, then only the extreme control points (P_0 and P_n) will belong to the boundary, and even they coincide with the corners (e.g., A, B), whereas the rest will be either inside or outside the domain Ω in accordance to the curvature of the curve AB .

3. The proposed global collocation procedure

3.1. General. For the given partial differential equation (PDE)

$$\frac{1}{c^2} \frac{\partial^2 u}{\partial t^2} - \nabla^2 u = 0 \quad \text{in } \Omega, \quad (12)$$

we seek an approximate solution to (12) which is a linear combination of the bivariate global *basis* functions $\{\phi_i(x, y)\}$, $i = 1, 2, \dots, q$:

$$\tilde{u}(x, y; t) = \sum_{j=1}^q \alpha_j(t) \cdot \phi_j(x, y). \quad (13)$$

Based on the global shape functions ϕ_j in (13), which are applied for the entire domain, we can apply either the proposed global collocation or the well-known Galerkin–Ritz method.

Without loss of generality, the boundary consists of \tilde{n}_1 breakpoints (which correspond to n_1 control points) under Dirichlet and \tilde{n}_2 ones (which correspond to n_2 control points) under Neumann boundary conditions. Although many acoustical cavities have absorbing boundaries (e.g., mufflers) with mixed boundary conditions (Robin-type) due to the acoustic impedance, for the sake of brevity below we limit the discussion in the two typical cases of boundary conditions, that is, open boundary (Dirichlet-type) and hard walls (Neumann-type).

3.2. The proposed global collocation approach. Fulfilling the PDE (12) at n_{col} collocation points, one obtains the matrix formulation (the index “ c ” stands for collocation)

$$[M_c]\{\ddot{a}(t)\} + [K_c]\{a(t)\} = \{0\}, \quad (14)$$

where

$$m_{ij}^c = \left(\frac{1}{c^2}\right)\phi_j(x_i), \quad k_{ij}^c = -\nabla^2\phi_j(x_i). \quad (15)$$

In (15), “ i ” corresponds to the collocation points and “ j ” to the control points. It can be noticed that in this formulation *no domain integral appears*. This advantage comes at the cost of having to calculate the stiffness elements k_{ij} through the two components of the Laplace operator in (15), which are given by

$$\begin{aligned} \frac{\partial^2\phi_j}{\partial x^2} &= \left(\frac{\partial\xi}{\partial x}\right)^2 \frac{\partial^2\phi_j}{\partial\xi^2} + 2\frac{\partial\xi}{\partial x}\frac{\partial\eta}{\partial x}\frac{\partial^2\phi_j}{\partial\xi\partial\eta} + \left(\frac{\partial\eta}{\partial x}\right)^2 \frac{\partial^2\phi_j}{\partial\eta^2} + \frac{\partial^2\xi}{\partial x^2}\frac{\partial\phi_j}{\partial\xi} + \frac{\partial^2\eta}{\partial x^2}\frac{\partial\phi_j}{\partial\eta}, \\ \frac{\partial^2\phi_j}{\partial y^2} &= \left(\frac{\partial\xi}{\partial y}\right)^2 \frac{\partial^2\phi_j}{\partial\xi^2} + 2\frac{\partial\xi}{\partial y}\frac{\partial\eta}{\partial y}\frac{\partial^2\phi_j}{\partial\xi\partial\eta} + \left(\frac{\partial\eta}{\partial y}\right)^2 \frac{\partial^2\phi_j}{\partial\eta^2} + \frac{\partial^2\xi}{\partial y^2}\frac{\partial\phi_j}{\partial\xi} + \frac{\partial^2\eta}{\partial y^2}\frac{\partial\phi_j}{\partial\eta}. \end{aligned} \quad (16)$$

The terms $\frac{\partial\xi}{\partial x}$, $\frac{\partial^2\xi}{\partial x^2}$, $\frac{\partial\xi}{\partial y}$ and $\frac{\partial^2\xi}{\partial y^2}$, as well as $\frac{\partial\eta}{\partial x}$, $\frac{\partial^2\eta}{\partial x^2}$, $\frac{\partial\eta}{\partial y}$ and $\frac{\partial^2\eta}{\partial y^2}$ in (16), are calculated as usual, starting from the inverse of the Jacobian matrix [Provatidis and Ioannou 2010, p. 400].

3.3. The well known Galerkin–Ritz approach. Applying the Galerkin method to (12), for the free vibration problem, one obtains the well known matrix formulation [Höllig 2003]

$$[\mathbf{M}]\{\ddot{\mathbf{a}}(t)\} + [\mathbf{K}]\{\mathbf{a}(t)\} = \{\mathbf{0}\}, \quad (17)$$

where $[\mathbf{M}]$ and $[\mathbf{K}]$ are the mass and stiffness matrices, respectively, which are given by

$$m_{ij} = \frac{1}{c^2} \int_{\Omega} \phi_i\phi_j d\Omega, \quad k_{ij} = \int_{\Omega} \nabla\phi_i\nabla\phi_j d\Omega. \quad (18)$$

A B-splines implementation in conjunction with Equations (17) and (18) is not a novel task, as the general procedure has been previously presented in a textbook ([Höllig 2003] and papers therein). For the completeness of our description, we should mention that

- (1) *Dirichlet* boundary conditions (near to $n_1 \leq n_{c,b}$ control points) are easily implemented eliminating both the n_1 rows and columns which correspond to the restrained coefficients;
- (2) *Neumann* boundary conditions (near to $n_2 \leq n_{c,b}$ control points) make the “near-boundary” (outer) control points be treated equally with the $n_{c,in}$ unrestrained internal ones. In the particular case of a *free-free* problem, *no* matrix elimination is required.

3.4. Implementation of boundary conditions in global collocation. In general, we fulfill the PDE applying (15) at n_{col} collocation points in the interior of the domain.

In free acoustic excitation, the collocation leads to the following general matrix equations system

$$[\mathbf{M}_{col,1} \quad \mathbf{M}_{col,2} \quad \mathbf{M}_{col,I}] \cdot \begin{bmatrix} \ddot{\mathbf{a}}_1 \\ \ddot{\mathbf{a}}_2 \\ \ddot{\mathbf{a}}_I \end{bmatrix} + [\mathbf{K}_{col,1} \quad \mathbf{K}_{col,2} \quad \mathbf{K}_{col,I}] \cdot \begin{bmatrix} \mathbf{a}_1 \\ \mathbf{a}_2 \\ \mathbf{a}_I \end{bmatrix} = \begin{bmatrix} \mathbf{F}_1 \\ \mathbf{0} \\ \mathbf{0} \end{bmatrix}, \quad (19)$$

where \mathbf{a}_1 and \mathbf{a}_2 are vectors of coefficients that refer to the above-mentioned n_1 and n_2 control points related to the boundary, respectively, while \mathbf{a}_I refers to the associated n_I “internal” (with respect to the reference square) control points.

3.4.1. Dirichlet boundary conditions. Dirichlet boundary conditions ($u = 0$) are easily applied. These conditions are readily implemented by eliminating the columns that correspond to the restricted nodes, that is, the matrices $\mathbf{M}_{\text{col},1}$ and $\mathbf{K}_{\text{col},1}$ in (19). In most cases this task is trivial, particularly when one or more entire sides, for example AB out of the whole boundary ($= AB \cup BC \cup CD \cup DA$), is restricted ($u = 0$). Obviously this happens because the boundary condition $u = 0$ along the side AB implies that all coefficients that correspond to it vanish ($a_i \equiv 0$). If the entire boundary is under Dirichlet conditions, then all relevant coefficients vanish (i.e., $\mathbf{a}_1 = \mathbf{0}$).

Therefore, eliminating the vectors $\mathbf{a}_1 = \ddot{\mathbf{a}}_1 = \mathbf{0}$, and assuming that no other part of the boundary is under Neumann conditions (\mathbf{a}_2 is absent), (19) becomes

$$\mathbf{M}_{\text{col},I} \cdot \ddot{\mathbf{a}}_I + \mathbf{K}_{\text{col},I} \cdot \mathbf{a}_I = \mathbf{0}. \tag{20}$$

Equation (20) depicts that the resulting matrices $\mathbf{M}_{\text{col},I}$ and $\mathbf{K}_{\text{col},I}$ will be square (of order $n_{c,\text{in}} \times n_{c,\text{in}}$) only when the number of collocation points equals the number of control points $n_{c,\text{in}}$ in the interior. Obviously, this condition is valid regardless of the multiplicity λ ($= 1$ or 2) of internal knots.

3.4.2. Neumann boundary conditions. Neumann boundary conditions ($\partial u / \partial \mathbf{n} = 0$, $\mathbf{n} =$ unit normal vector) impose a linear dependency between the coefficients associated to the control points in the neighborhood of the boundary. A similar dependency had been previously found, however in conjunction with Lagrange polynomials [Provatidis 2008a, p. 245]. In this way, the matrix elements in those columns related to the free boundary are first reorganized and then condensed; details will be given below.

Taking the first derivative of (13) with respect to the unit normal vector \mathbf{n} (at a boundary point), we obtain

$$\frac{\partial u}{\partial \mathbf{n}} = \sum_{k=1}^q \frac{\partial \phi_k(\xi, \eta)}{\partial \mathbf{n}} \cdot a_k. \tag{21}$$

In the sum that appears in (21), $n_{c,\text{in}}$ out of the total number of q control points belong to the interior, while n_2 belong to the boundary (actually they are outside or inside the domain in accordance to the curvature). For a *smooth* boundary, applying (21) to n_2 boundary points (in the neighborhood of the “close-to-the-boundary” control points), we derive the matrix equation

$$\begin{bmatrix} \underbrace{\mathbf{B}_{22}}_{n_2 \times n_2} & \underbrace{\mathbf{B}_{2I}}_{n_2 \times n_I} \end{bmatrix} \cdot \begin{bmatrix} \mathbf{a}_2 \\ \mathbf{a}_I \end{bmatrix} = \begin{bmatrix} \mathbf{0} \\ \mathbf{0} \end{bmatrix}. \tag{22}$$

Eliminating \mathbf{a}_2 from (22) and substituting into (19) in which the vector \mathbf{a}_1 is absent, we obtain

$$\mathbf{M}^* \ddot{\mathbf{a}}_I + \mathbf{K}^* \mathbf{a}_I = \mathbf{0}, \tag{23}$$

where

$$\mathbf{M}^* = \mathbf{M}_{\text{col},I} - \mathbf{M}_{\text{col},2} \mathbf{B}_{22}^{-1} \mathbf{B}_{2I}, \quad \mathbf{K}^* = \mathbf{K}_{\text{col},I} - \mathbf{K}_{\text{col},2} \mathbf{K}_{22}^{-1} \mathbf{K}_{2I}. \tag{24}$$

The imposition of Neumann boundary conditions in the case of nonsmooth boundary (e.g., corners appearing in a rectangular $ABCD$ like that of Example 1, free-free boundary conditions) is performed as follows. We select two opposite sides, for example AD and BC and impose the Neumann boundary conditions at so many points along each of them as the number of the corresponding control points (the end points (A, D) of the side AD , and (B, C) of BC are included). For the remaining two sides, AB

and CD , the corner points are excluded, therefore for each of them Neumann boundary conditions are applied to as many boundary points as the corresponding number of control points minus two. This is the minimum number of Neumann boundary conditions that can be applied in a straightforward manner. However, if one wishes to apply Neumann boundary conditions at the ends of the sides AB and CD as well, then the number of rows in (22) will increase by four, thus a least-squares procedure should be applied to it in order to make possible the inversion of matrix \mathbf{B}_{22} .

3.4.3. Implementation to static problems. At this point, it is instructive to refresh those basics of the collocation method related to nonhomogeneous boundary conditions for solving boundary value problems. Details for the one-dimensional problem defined in the interval $[0, L]$ are given in Appendix A.

3.4.4. Multiplicity of internal knots. As mentioned in Section 2.3, after the breakpoints along the boundary are given, the next decisive step is to assign the multiplicity of internal knots.

In the case of $\lambda = 2$, in conjunction with $p = 3$, the golden rule is to take the collocation points at the 2×2 Gauss points in the $(n_x \times n_y)$ cells formed by the breakpoints, so that the number of equations equals the number of unknowns, always related to the internal control points. For $p > 3$, the same occurs when $\lambda = p - 1$, whereas the aforementioned 2×2 is replaced by a $(p - 1) \times (p - 1)$ Gaussian quadrature.

In contrast, when $\lambda = 1$, in conjunction with $p = 3$, we can use more collocation points, for example, the same as those for $\lambda = 2$. In such case the matrices $\mathbf{M}_{\text{col},I}$ and $\mathbf{K}_{\text{col},I}$ are nonsquare. For $p > 3$, we can use the same as those for $\lambda = p - 1$ or smaller. This shortcoming is easily resolved applying the least-squares technique, of which the academic implementation is to left-multiply (20) by the transpose of the matrix $\mathbf{M}_{\text{col},I}$, thus leading to

$$\underbrace{\bar{\mathbf{M}}}_{n_I \times n_I} \ddot{\mathbf{a}}_I + \underbrace{\bar{\mathbf{K}}}_{n_I \times n_I} \mathbf{a}_I = \mathbf{0}, \quad (25)$$

where

$$\bar{\mathbf{M}} = (\mathbf{M}_{\text{col},I})^T \cdot (\mathbf{M}_{\text{col},I}), \quad \bar{\mathbf{K}} = (\mathbf{M}_{\text{col},I})^T \cdot (\mathbf{K}_{\text{col},I}). \quad (26)$$

In the case of adopting $\lambda = 1$ ($C^{p-\lambda}$ -continuity), another possibility is to collocate at the images of the Demko's or Greville's abscissae [Auricchio et al. 2010; de Boor 2001, p. 192], thus skipping the above-mentioned least-squares procedure. For the sake of brevity, in this paper a relevant choice is characterized by the term "isogeometric" collocation.

3.4.5. Eigenvalues extraction. It can be noticed that (20) and (23) have the form of a standard problem in dynamics and therefore can be calculated either taking the roots of the characteristic polynomial produced by demanding that $\det(\|\mathbf{K} - \lambda\mathbf{M}\|) = 0$, or by any established algorithm for nonsymmetric matrices such as QR .

4. Numerical implementation

4.1. Global collocation method. The proposed global collocation method was implemented using $(p - 1)$ Gauss points per direction, between any two successive breakpoints. In the tensor product, the breakpoints create $n_x \times n_y$ cells. Using $(p - 1)^2$ collocation points per cell, the total number of collocation points becomes $n_{\text{col}} = (p - 1)^2 n_x n_y$, which equals to the number of unknown coefficients.

Clearly, in the case of multiple double knots (e.g., $\lambda = 2$ for $p = 3$) the total number of control points (coefficients) in the tensor product is $q = 4(n_x + 1) \times (n_y + 1)$, of which $n_b = 4(n_x + n_y + 1)$ control points (coefficients) lie on the boundary.

- For a *Dirichlet* problem (e.g., with $p = 3$), the aforementioned n_b columns are eliminated, thus $n_{\text{int}} = q - n_b = 4n_x n_y$ coefficients remain (they correspond to the control points in the interior). Therefore, the number of the collocation points n_{col} equals to the number of unknown coefficients, a fact that leads to a square matrix of unknowns which can be easily solved.
- For a *free-free* problem, all coefficients that correspond to the boundary control points are again eliminated, thus resulting in $n_{\text{int}} = q - n_b = 4n_x n_y$, exactly the same number as in the above-mentioned Dirichlet problem.

Also, in case of simple knots ($\lambda = 1$), in conjunction with $p = 3$, the total number of control points (coefficients) in the tensor product is $q = (n_x + 3) \times (n_y + 3)$, of which $n_b = 2(n_x + n_y + 4)$ control points (coefficients) lie on the boundary. As previously, in both Dirichlet and Neumann problems all the coefficients associated to the n_b close-to-boundary control points are eliminated thus $n_{\text{int}} = q - n_b = 4n_x n_y$ coefficients remain and constitute the order of the final matrices.

Moreover, for any chosen multiplicity λ , in conjunction with a chosen number of breakpoint subdivisions, the number q of control points is determined according to (7). In addition to the above schemes, instead of using only Gaussian points this study reports about numerical experience using the images of Demko's and Greville's abscissae for collocating points, previously applied in isogeometric analysis [Auricchio et al. 2010].

4.2. Galerkin–Ritz global method. The elements m_{ij} of the mass matrix are products of two basis functions, each of piecewise p -th (i.e., third) degree. In the particular case of a rectangular domain, the integrand becomes of piecewise sixth degree, thus it requires four-point Gauss quadrature per direction, that is, sixteen Gauss points per integration cell. For $p > 3$, we use $(p + 1) \times (p + 1)$ Gauss points per integration cell.

A Dirichlet problem, for $p = 3$, leads to mass and stiffness matrices of order $n_{\text{int}} = q - n_b = 4n_x n_y$, while a Neumann problem leads to matrices of order $n_{\text{eq}} = 4(n_x + 1) \times (n_y + 1)$, a fact that is entirely different from the above-mentioned collocation technique.

5. Numerical examples

A Matlab code was developed on a standard PC Pentium IV. The basis functions $N_{i,p}$ and their derivatives were created using the “spcol” function, which exists in the Spline Toolkit. Demko's abscissae were determined using the “chbpnt” function. The eigenvalues were calculated using the standard “eig” function.

The theory is now elucidated by two examples taken from the literature [Provatidis 2004; 2009a], in which the exact analytical solution is known. The quality of the numerical solution \tilde{u} is evaluated in terms of the relative error, which was calculated as

$$e_r = \frac{\tilde{u} - u_{\text{exact}}}{u_{\text{exact}}} \times 100\%. \quad (27)$$

Mode (m, n) Exact ω^2			Error (in %) of calculated eigenvalues											
			Collocation								Galerkin–Ritz			
			(a) $\lambda = 2$ $(n_x \times n_y)$				(b) $\lambda = 1$ $(n_x \times n_y)$				(c) $\lambda = 1$ $(n_x \times n_y)$			
			2 × 1	4 × 2	6 × 3	8 × 4	2 × 1	4 × 2	6 × 3	8 × 4	2 × 1	4 × 2	6 × 3	8 × 4
1	(0, 0)	0	—	—	—	—	—	—	—	—	—	—	—	—
2	(1, 0)	1.5791	0.23	0.02	0.00	0.00	0.26	0.02	0.00	0.00	0.06	0.00	0.00	0.00
3	(2, 0)	6.3165	−8.81	0.23	0.05	0.02	−8.81	0.26	0.05	0.02	0.10	0.09	0.01	0.00
4	(0, 1)	8.1567	−8.81	0.23	0.05	0.02	−8.81	0.26	0.05	0.02	0.06	0.06	0.00	0.00
5	(1, 1)	9.7358	−7.35	0.19	0.04	0.01	−7.34	0.22	0.04	0.01	0.06	0.05	0.00	0.00
6	(3, 0)	14.2122	−7.14	0.67	0.23	0.08	−7.14	1.83	0.26	0.08	1.91	1.91	0.10	0.01
7	(2, 1)	14.4732	10.35	0.23	0.05	0.02	—	0.26	0.05	0.02	88.07	0.65	0.00	0.00
8	(3, 1)	22.3689	4.65	0.51	0.16	0.06	—	1.26	0.19	0.06	58.17	1.61	0.07	0.01
9	(4, 0)	25.2662	—	−8.81	0.55	0.23	—	−8.81	1.01	0.26	93.83	0.12	1.01	0.11
10	(0, 2)	32.6268	—	−8.81	0.55	0.23	—	−8.81	1.01	0.26	51.98	0.10	0.84	0.09
Number of equations			8	32	72	128	6	15	28	45	20	35	54	77

Table 1. Example 1: calculated eigenvalues of a rectangular acoustic cavity ($a = 2.5$ m, $b = 1.1$ m) under *Neumann* (free-free: $\partial u/\partial n = 0$) boundary conditions, using various $n_x \times n_y$ uniform subdivisions in conjunction with cubic B-splines ($p = 3$). Results are shown as percentage errors for an approximation involving “tensor product B-splines” using three alternative formulations: (a) *collocation* (with multiplicity $\lambda = 2$), (b) *collocation* (with multiplicity $\lambda = 1$), and (c) *Galerkin–Ritz* (with multiplicity $\lambda = 1$).

Example 1: eigenvalues of rectangular acoustical cavity. We consider a rectangular acoustical cavity of dimensions $a = 2.5$ m, $b = 1.1$ m with sound velocity $c = 1$ m/s. Two types of boundary conditions are considered: (a) *Neumann* (free-free), and (b) *Dirichlet* boundary conditions, for which the exact analytical eigenvalues are given by

$$\text{Free-free: } \omega_{mn}^2 = \pi^2 c^2 \left(\frac{m^2}{a^2} + \frac{n^2}{b^2} \right), \quad m, n = 0, 1, 2, \dots, \tag{28}$$

$$\text{Dirichlet: } \omega_{mn}^2 = \pi^2 c^2 \left(\frac{m^2}{a^2} + \frac{n^2}{b^2} \right), \quad m, n = 1, 2, \dots \tag{29}$$

In all cases a uniform mesh of $(n_x \times n_y)$ subdivisions of breakpoints along x - and y -directions, respectively, has been used. The obtained results for $p = 3$ are shown in Tables 1–3. In more detail:

- (1) Table 1 shows the results for *Neumann* boundary conditions, for three different formulations, that is, B-splines collocation in conjunction with the usual multiplicity $\lambda = 2$ and the novel $\lambda = 1$, as well as B-splines Galerkin–Ritz with the usual multiplicity $\lambda = 1$. It can be noticed that both formulations are of similar quality. The proposed collocation method requires the most degrees of freedom when $\lambda = 2$ and the least when $\lambda = 1$.
- (2) Table 2 shows the results for *Dirichlet* boundary conditions, again for previous three different formulations. It can be noticed that again the proposed collocation and the Galerkin–Ritz are of the same quality. It can be also noticed that the alternative least-squares collocation ($\lambda = 1$) is almost

Mode (m, n) Exact ω^2			Error (in %) of calculated eigenvalues											
			Collocation								Galerkin-Ritz			
			(a) $\lambda = 2$ ($n_x \times n_y$)				(b) $\lambda = 1$ ($n_x \times n_y$)				(c) $\lambda = 1$ ($n_x \times n_y$)			
			2 × 1	4 × 2	6 × 3	8 × 4	2 × 1	4 × 2	6 × 3	8 × 4	2 × 1	4 × 2	6 × 3	8 × 4
1	(1, 1)	9.7358	18.12	0.19	0.04	0.01	18.12	0.19	0.04	0.01	1.11	0.02	0.01	0.00
2	(2, 1)	14.4732	21.59	0.23	0.05	0.02	25.38	0.24	0.05	0.02	3.53	0.06	0.01	0.00
3	(3, 1)	22.3689	15.74	0.51	0.16	0.06	15.74	0.67	0.18	0.06	4.36	0.45	0.07	0.01
4	(4, 1)	33.4229	-6.25	16.37	0.43	0.17	-6.25	31.89	0.64	0.20	8.58	8.58	0.57	0.09
5	(1, 2)	34.2059	-3.65	20.59	0.52	0.22	11.04	36.69	0.58	0.24	21.12	15.69	0.20	0.09
6	(2, 2)	38.9433	-3.88	18.12	0.47	0.19	17.41	25.40	0.52	0.21	27.85	5.37	0.18	0.08
7	(3, 2)	46.8390	-2.38	11.03	0.45	0.18	—	20.44	0.50	0.20	—	4.66	0.18	0.07
8	(5, 1)	47.6351	10.83	13.31	0.42	0.39	—	19.34	1.13	0.55	—	9.00	1.95	0.46
9	(4, 2)	57.8930	—	21.59	0.55	0.23	—	40.06	0.70	0.25	—	14.22	0.45	0.11
10	(6, 1)	65.0056	—	10.85	11.50	0.59	—	29.34	12.05	1.21	—	20.72	12.46	1.59
Number of equations			8	32	72	128	6	15	28	45	6	15	28	45

Table 2. Example 1: calculated eigenvalues of a rectangular acoustic cavity ($a = 2.5$ m, $b = 1.1$ m) under *Dirichlet* ($u = 0$) boundary conditions, using various $n_x \times n_y$ uniform subdivisions in conjunction with cubic B-splines ($p = 3$). Results are shown as percentage errors for an approximation involving “tensor product B-splines” using three alternative formulations: (a) *collocation* (with multiplicity $\lambda = 2$), (b) *collocation* (with multiplicity $\lambda = 1$), and (c) *Galerkin-Ritz* (with multiplicity $\lambda = 1$).

Mode		Error (in %) of calculated eigenvalues							
		Conventional finite elements (FEM)							
		(a) Free-free ($n_x \times n_y$)				(b) Dirichlet ($n_x \times n_y$)			
		2 × 1	4 × 2	6 × 3	8 × 4	2 × 1	4 × 2	6 × 3	8 × 4
1		—	—	—	—	—	18.93	8.27	4.60
2		21.59	5.24	2.30	1.29	—	21.59	9.43	5.24
3		21.59	21.59	9.43	5.24	—	35.00	17.15	9.54
4		21.59	21.59	9.43	5.24	—	—	30.11	17.60
5		21.59	18.93	8.27	4.60	—	—	35.19	20.65
6		23.82	23.82	11.44	7.17	—	—	32.35	18.93
7		—	40.13	19.39	9.98	—	—	32.17	18.68
8		—	35.00	17.15	9.54	—	—	38.13	28.29
9		—	21.59	36.78	21.59	—	—	36.78	21.59
10		—	21.59	33.28	20.47	—	—	56.14	38.00
Number of equations		6	15	28	45	0	3	10	21

Table 3. Example 1: calculated eigenvalues of a rectangular acoustic cavity ($a = 2.5$ m, $b = 1.1$ m) using various $n_x \times n_y$ uniform subdivisions. Results are shown as percentage errors for conventional bilinear (four-node) finite elements under (a) free-free and (b) Dirichlet boundary conditions.

identical with the orthogonal collocation ($\lambda = 2$) and even it has the same (small) number of control points as the Galerkin–Ritz formulation.

- (3) For comparison, Table 3 shows the results obtained using conventional finite elements—for the same mesh density, of course. It can be noticed that the minor differences appearing in Table 1 and Table 2 are negligible, that is, of the same order of accuracy when compared with the conventional finite element solution in Table 3. However, for the same number of breakpoints, the number of DOFs in the conventional FEM is minimal.

In the sequence, the results of Tables 1–3 are enhanced as follows. First, the discretization of breakpoints is extended from 8×4 to 12×6 , 16×8 and 32×16 at maximum. Second, three additional collocation schemes from recent literature were tested, involving, in order, Demko’s, Greville’s T_n - and Greville’s S_{n+2} abscissae (for definitions see [Auricchio et al. 2010]).

Comparative results for $p = 3$ and *Neumann* boundary conditions are shown in Figure 1, where one can

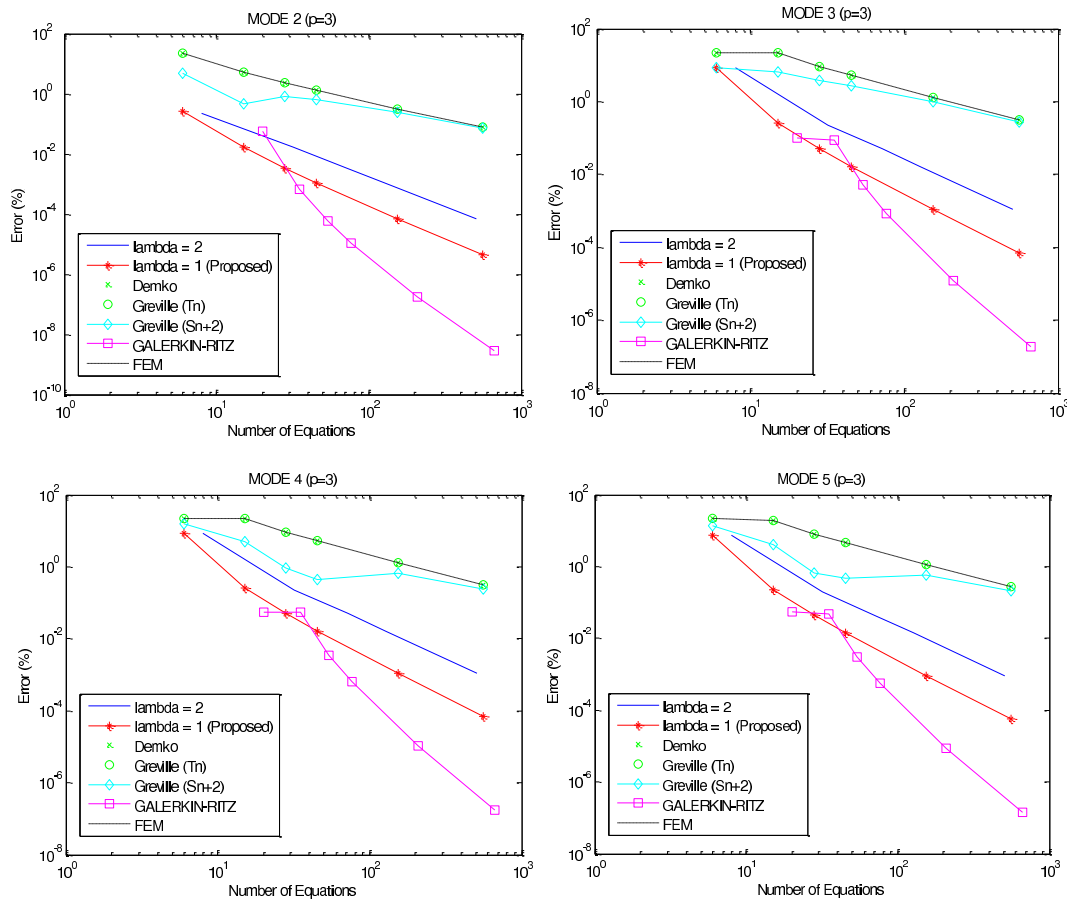


Figure 1. Rectangular under *Neumann* boundary conditions: Convergence of the first four nonzero eigenvalues, ω_i^2 , $i = 2, 3, 4, 5$, in terms of number of equations using cubic B-splines, $p = 3$ (the first eigenvalue, not shown, equals to zero: $\omega_1^2 = 0$).

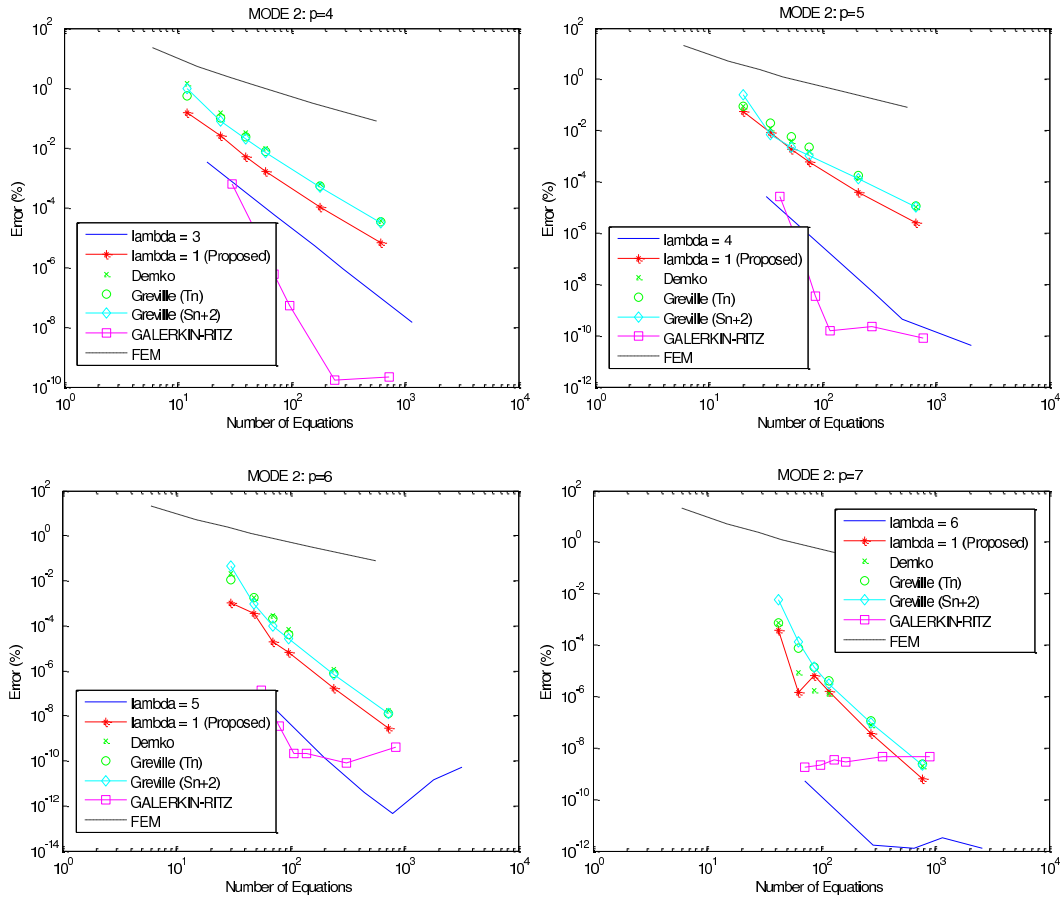


Figure 2. Rectangular under *Neumann* boundary conditions: convergence of the second eigenvalue, ω_2^2 , in terms of number of equations, for higher polynomial degrees ($p = 4, 5, 6$ and 7).

notice the overall superiority of the Galerkin–Ritz B-splines method, in terms of accuracy. The proposed single knot based ($\lambda = 1$) least-squares collocation closely follows the accuracy of Galerkin–Ritz method, whereas the usual double knot based ($\lambda = 2$) collocation method is of adequate accuracy. Moreover, the images of Demko’s and Greville’s abscissae as collocation points lead to rather poor results. Surprisingly, Demko’s solution coincides with the conventional FEM solution (based on 4-node bilinear elements) up to the twelfth decimal point at least.

For the same (*Neumann*) boundary conditions, the superiority of the proposed method ($\lambda = 1$) does not continue when dealing with higher polynomial degrees ($p = 4, 5, 6$ and 7), where the choice of multiplicity $\lambda = p - 1$ outperforms between all collocation methods tested in this study (Figure 2).

Comparative results for $p = 3$ and *Dirichlet* boundary conditions are shown in Figure 3, where one can again notice the overall superiority of the Galerkin–Ritz B-splines method, in terms of accuracy. The proposed single knot based ($\lambda = 1$) least-squares collocation is again the best accurate scheme between all tested collocation methods. Moreover, the images of Demko’s and Greville’s (T_n -based) abscissae as

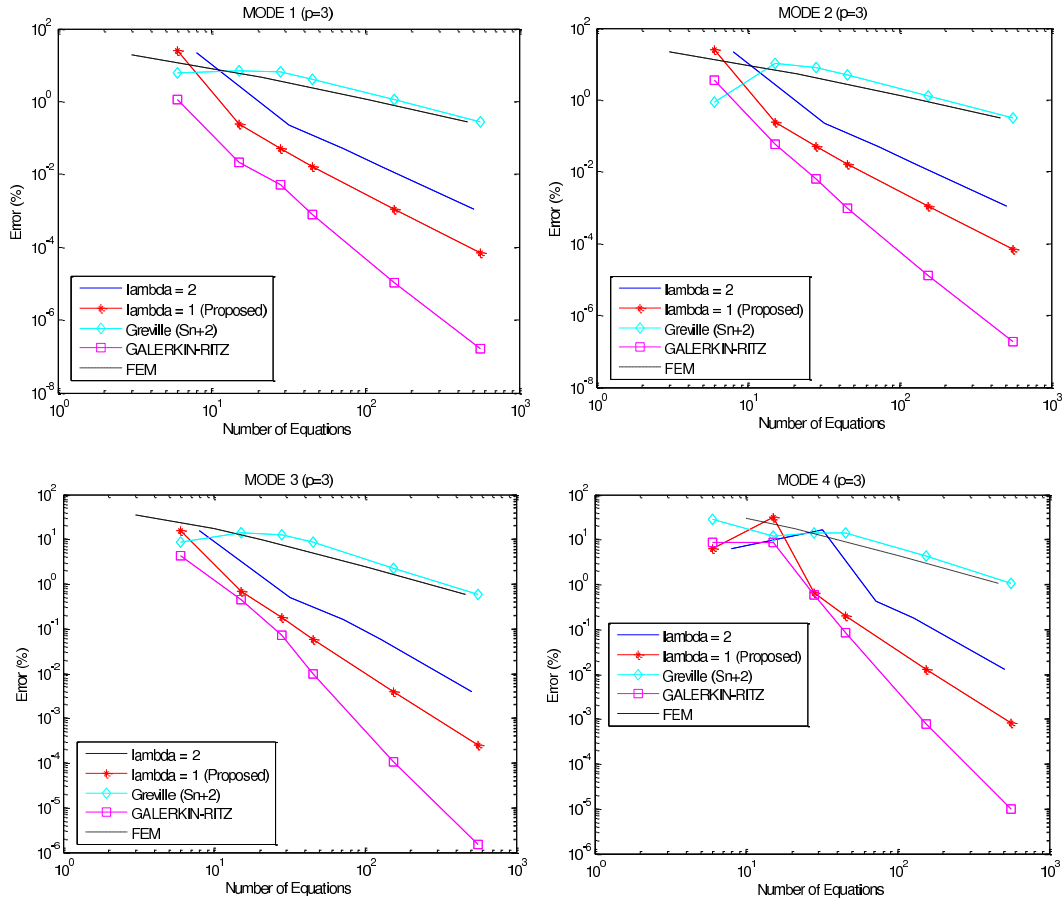


Figure 3. Rectangular under *Dirichlet* boundary conditions: convergence of the first four eigenvalues, ω_i^2 , $i = 1, 2, 3, 4$, in terms of number of equations using cubic B-splines ($p = 3$).

collocation points are not applicable as they lead to singular dynamic matrices. This finding is justified by the fact that the *extreme* collocation points of these two sets *belong* to the boundary and therefore Dirichlet boundary conditions erase the dominating diagonal terms appearing in series expansion given by (13). Only the Greville's (S_{n+2} -based) abscissae are applicable but the quality of results is slightly lower compared even with the conventional FEM solution (4-node bilinear elements).

For the same (Dirichlet) boundary conditions, the superiority of the proposed method ($\lambda = 1$) does not continue when dealing with higher polynomial degrees ($p = 4, 5, 6$ and 7), where the choice of multiplicity $\lambda = p - 1$ outperforms between all collocation methods tested in this study (Figure 4). Concerning the other (isogeometric) sets of global collocation, only the images of Greville's (S_{n+2} -based) abscissae are applicable and of similar quality with the proposed least-squares scheme.

Example 2: eigenvalues of circular acoustical cavity. A circular cavity of radius $a = 1$ m under Dirichlet or Neumann (free-free) conditions is considered. For the purposes of this study, a unit reference sound

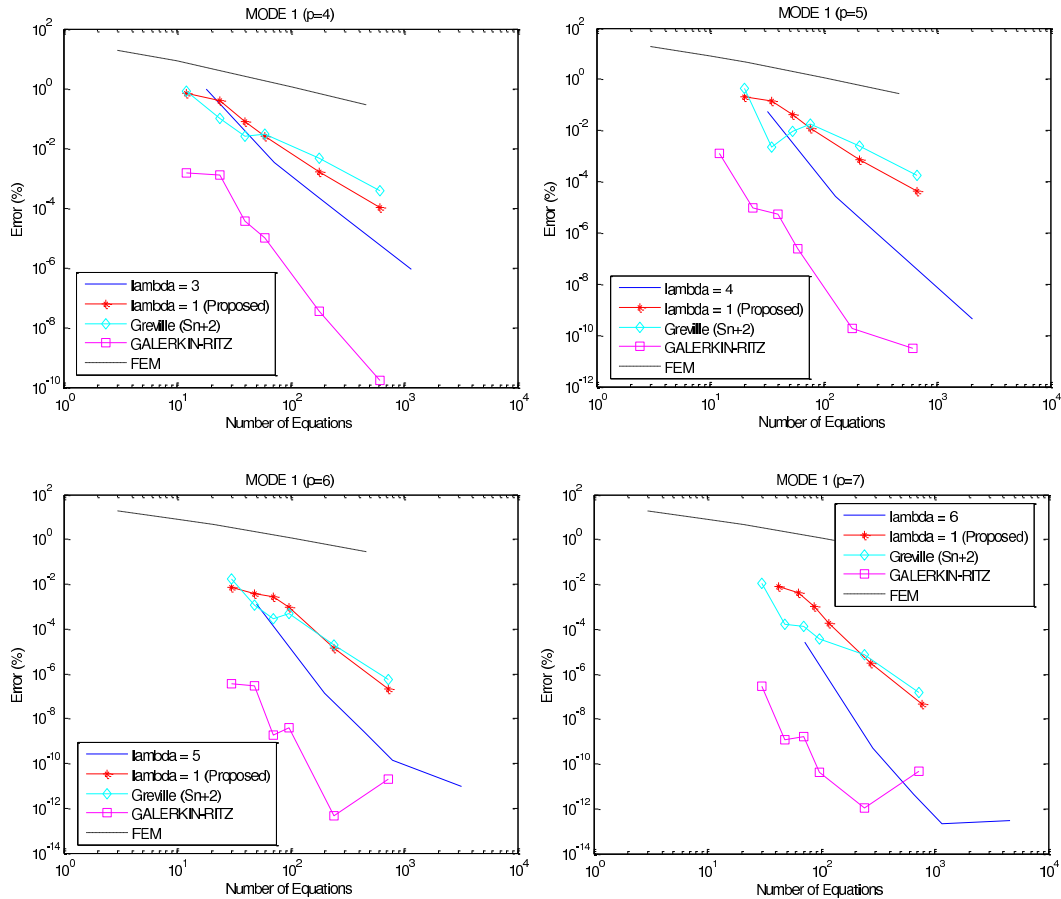


Figure 4. Rectangular under *Dirichlet* boundary conditions: convergence of the first eigenvalue, ω_1^2 , in terms of number of equations, for higher polynomial degrees ($p = 4, 5, 6$ and 7).

velocity, $c = 1$ m/s, is considered. The theoretical eigenvalues are given by the formula

$$\text{Dirichlet: } J_m(ka) = 0, \quad m = 0, 1, 2, \dots, \tag{30}$$

$$\text{Free-free (Neumann): } J'_m(ka) = 0, \quad m = 0, 1, 2, \dots, \tag{31}$$

where $J'_m(ka)$ is the first derivative of the Bessel function $J_m(ka)$ of the first kind and order m and $k = \omega/c$ the wavenumber.

Now the discretization consists of 4, 8, 16, and 32 breakpoints uniformly distributed along the entire circumference. This corresponds to $n_x = n_y = n = 1, 2, 4$ and 8 , subdivisions of every side in the reference square $ABCD$, respectively. As previously, the control points for $p = 3$ were derived for multiplicity $\lambda = 1$ and 2 .

Tables 4 and 5 show the results for the Dirichlet and Neumann problems, respectively. It can be noticed that for medium and fine meshes the results are of similar quality, especially when they are compared with conventional finite elements. The latter elements have been previously studied in [Provatis 2004,

Mode m Exact ω^2			Error (in %) of calculated eigenvalues											
			Collocation								Galerkin–Ritz			
			(a) $\lambda = 2$				(b) $\lambda = 1$				(c) $\lambda = 1$			
			Number of subdivisions ($4n$)				Number of subdivisions ($4n$)				Number of subdivisions ($4n$)			
			4	8	16	32	4	8	16	32	4	8	16	32
1	0	5.7832	97.14	-3.48	0.00	0.00	98.68	-3.70	0.02	0.00	8.94	-0.01	0.01	0.00
2	1	14.6820	39.25	16.63	0.13	0.01	38.98	47.78	0.68	0.01	16.72	11.55	0.46	0.00
3	1	14.6820	39.25	16.63	0.13	0.01	38.98	47.78	0.68	0.01	16.72	11.55	0.46	0.00
4	2	26.3746	-1.59	21.84	-2.23	0.03	-2.54	34.75	-2.20	0.03	29.88	11.97	0.30	0.01
5	2	26.3746	—	33.12	0.88	0.07	—	49.23	3.38	0.09	—	30.32	2.02	0.02
6	0	30.4713	—	27.51	-3.31	0.05	—	195.80	-3.35	0.07	—	26.45	0.16	0.03
7	3	40.7065	—	9.04	-0.20	0.14	—	246.60	2.66	0.19	—	65.18	4.81	0.07
8	3	40.7065	—	9.04	-0.20	0.14	—	246.60	2.66	0.19	—	65.18	4.81	0.07
9	1	49.2185	—	23.30	11.63	0.14	—	327.16	13.92	0.23	—	121.01	20.60	0.17
10	1	49.2185	—	23.30	15.74	0.14	—	—	80.75	0.23	—	—	32.95	0.17
No. of equations			4	16	64	256	4	9	25	81	4	9	25	81

Table 4. Example 2: calculated eigenvalues of a circular acoustic cavity of radius 1.0 m under *Dirichlet* ($u = 0$) boundary conditions, using various uniform subdivisions in conjunction with cubic B-splines ($p = 3$). Results are shown as percentage errors for “tensor product B-splines” approximation using three alternative formulations: (a) *collocation* (with multiplicity $\lambda = 2$), (b) *collocation* (with multiplicity $\lambda = 1$), and (c) *Galerkin–Ritz* (with multiplicity $\lambda = 1$).

Mode m Exact ω^2			Error (in %) of calculated eigenvalues											
			Collocation								Galerkin–Ritz			
			(a) $\lambda = 2$				(b) $\lambda = 1$				(c) $\lambda = 1$			
			Number of subdivisions ($4n$)				Number of subdivisions ($4n$)				Number of subdivisions ($4n$)			
			4	8	16	32	4	8	16	32	4	8	16	32
1	0	0.00	—	—	—	—	—	—	—	—	—	—	—	—
2	1	3.3900	-15.28	1.89	0.05	0.00	-15.04	4.27	-0.06	-0.01	0.09	0.29	0.00	0.00
3	1	3.3900	-15.28	1.89	0.05	0.00	-15.04	4.27	-0.06	-0.01	0.09	0.29	0.00	0.00
4	2	9.3284	-43.16	-9.76	-0.17	-0.06	-43.64	-9.77	-0.58	-0.10	-1.13	0.18	0.06	0.00
5	2	9.3284	—	8.61	0.18	0.00	—	23.17	0.42	0.01	50.37	2.71	0.09	0.00
6	0	14.6820	—	-8.50	0.36	0.03	—	-8.81	0.57	0.03	68.85	0.50	0.15	0.00
7	3	17.6500	—	0.44	0.09	-0.08	—	13.95	1.06	-0.11	63.78	9.68	0.76	0.00
8	3	17.6500	—	0.44	0.09	-0.08	—	13.95	1.06	-0.11	63.78	9.68	0.76	0.00
9	4	28.2764	—	-9.27	-2.09	-0.27	—	-1.97	-1.66	-0.43	67.23	9.80	0.45	0.02
10	4	28.2764	—	1.29	2.83	-0.01	—	—	9.40	0.14	90.50	88.13	5.17	0.03
Number of equations			4	16	64	256	4	9	25	81	16	25	49	121

Table 5. Example 2: calculated eigenvalues of a circular acoustic cavity of radius 1.0 m under *Neumann* (free-free) boundary conditions, using various uniform subdivisions in conjunction with cubic B-splines ($p = 3$). See caption of previous table for details.

p. 51]; briefly, for the Neumann problem in conjunction with 216 triangular elements and 127 nodes, the error in the first three nonrigid modes was: $\cong 0.86\%$, 1.36% , and 1.79% , respectively.

Better insight is obtained when increasing mesh density into 40 breakpoints and again comparing all those methods tested in Example 1. Concerning the FEM, the same mesh with that of breakpoints considered in collocation methods was used. The results are as follows.

For the *Dirichlet* problem, it is clearly shown in Figure 5 that B-splines Galerkin–Ritz method outperforms and then the proposed collocation method ($\lambda = 1$) follows. The images of Demko’s and Greville’s (T_n -based) abscissae lead to singular matrices, whereas Greville’s (S_{n+2} based) abscissae work well but perform slightly worse even than usual FEM.

For the *Neumann* problem, it is clearly shown in Figure 6 that B-splines Galerkin–Ritz method again outperforms and then the proposed collocation method ($\lambda = 1$) follows. The images of Demko’s and Greville’s (T_n -based) abscissae do not now lead to singular matrices but the errors are tremendously high (some eigenvalues are even negative), whereas Greville’s (S_{n+2} -based) abscissae again work well but in some cases hardly fight the FEM solution.

6. Discussion

The global B-spline collocation method has been previously applied in the 1960s mainly in 1D elliptic problems [de Boor 2001], whereas preliminary eigenvalue analysis has been discussed by Jerome and Varga [1969]. Collocation methods have been extensively used for 2D problems but they have been implemented mostly in conjunction with small size elements; for details we refer to [Provatidis 2009b] and papers therein. For cubic B-splines, the state-of-the-art is to use two collocation points between two successive breakpoints (per direction). The latter matter is closely related to double knots (multiplicity of internal knots equal to two: $\lambda = 2$), so as to produce as many equations as the number of the unknown coefficients. In contrast, Galerkin–Ritz is usually applied on the basis of multiplicity of internal knots equal to one ($\lambda = 1$) [Höllig 2003] (for the sake of brevity in this study the case of double knots was not tested).

In the part of this study concerning cubic piecewise polynomials ($p = 3$), we found that the B-splines based global collocation method is applicable for any multiplicity of internal knots, that is, the usual ($\lambda = 2$) and the new ($\lambda = 1$). For the latter case ($\lambda = 1$), in which n_x subdivisions of breakpoints per direction lead to $n_x + 3$ control points, we have initially tested to collocate at the centroids of the n_x cells defined by the breakpoints plus the ends and the middle of the domain in the corresponding direction, ξ or η . Although in this way we derived as many equations as the number of the coefficients, the results were not satisfactory. In contrast, when the collocation was performed taking 2×2 (Gauss) points per cell, that is exactly the same as those used in case ($\lambda = 2$), the results became of equal quality as in case ($\lambda = 2$). The increased number of equations, compared to the smaller number of control points (and associated coefficients), was easily resolved applying a *least-squares* reduction of them (left-multiplication by a transpose matrix) thus producing a matrix of order equal to the number of control points.

From the study of Example 1 it is concluded that the use of images of Greville (S_{n+2} -based) abscissae is a good choice when applied in conjunction with polynomials of higher degree ($p > 3$). The images of Demko and Greville (T_n -based) abscissae must never be applied to Dirichlet-type eigenvalue problems in acoustics.

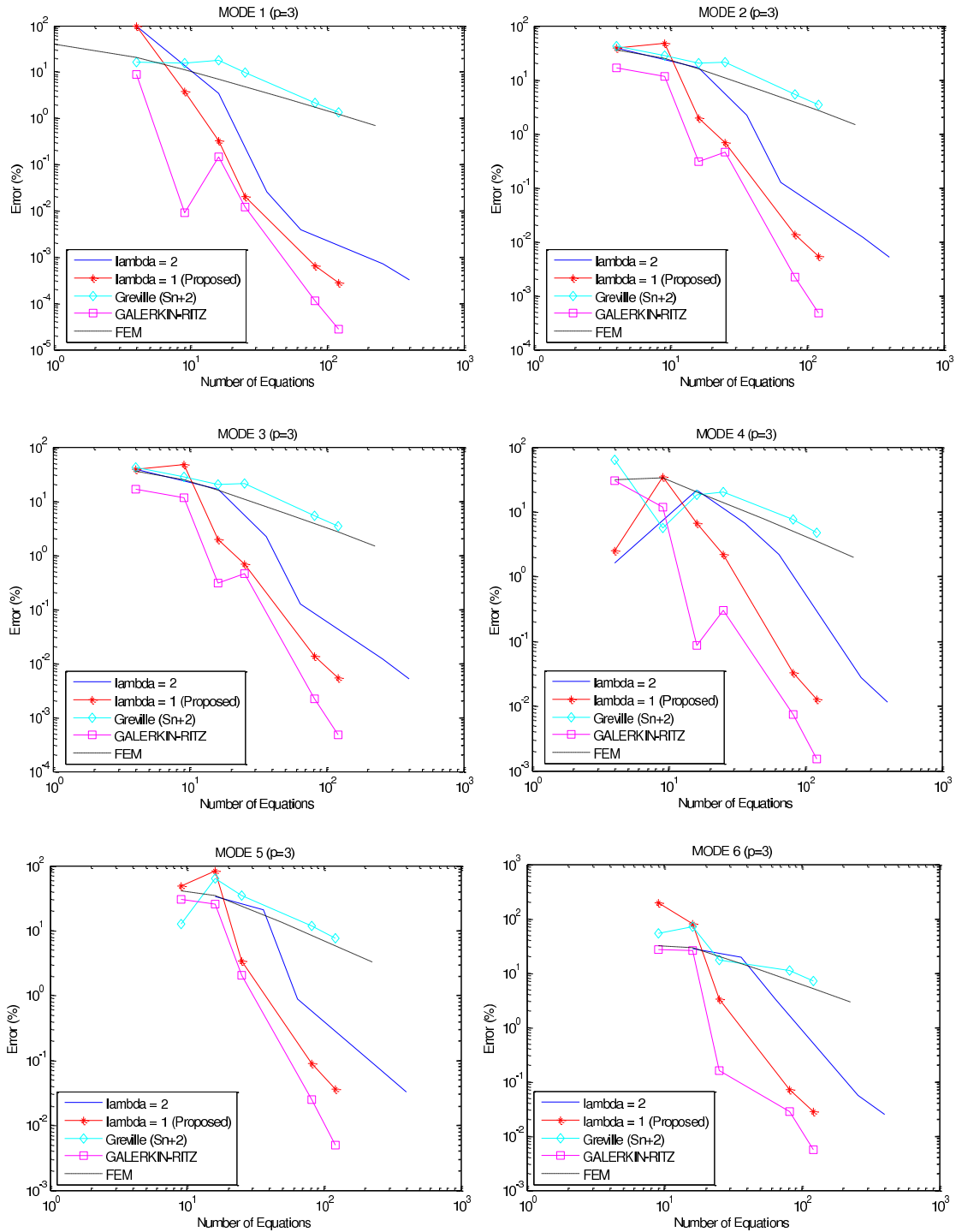


Figure 5. Circular cavity under *Dirichlet* boundary conditions: convergence of the first six eigenvalues in terms of number of equations, for cubic B-splines interpolation ($p = 3$).

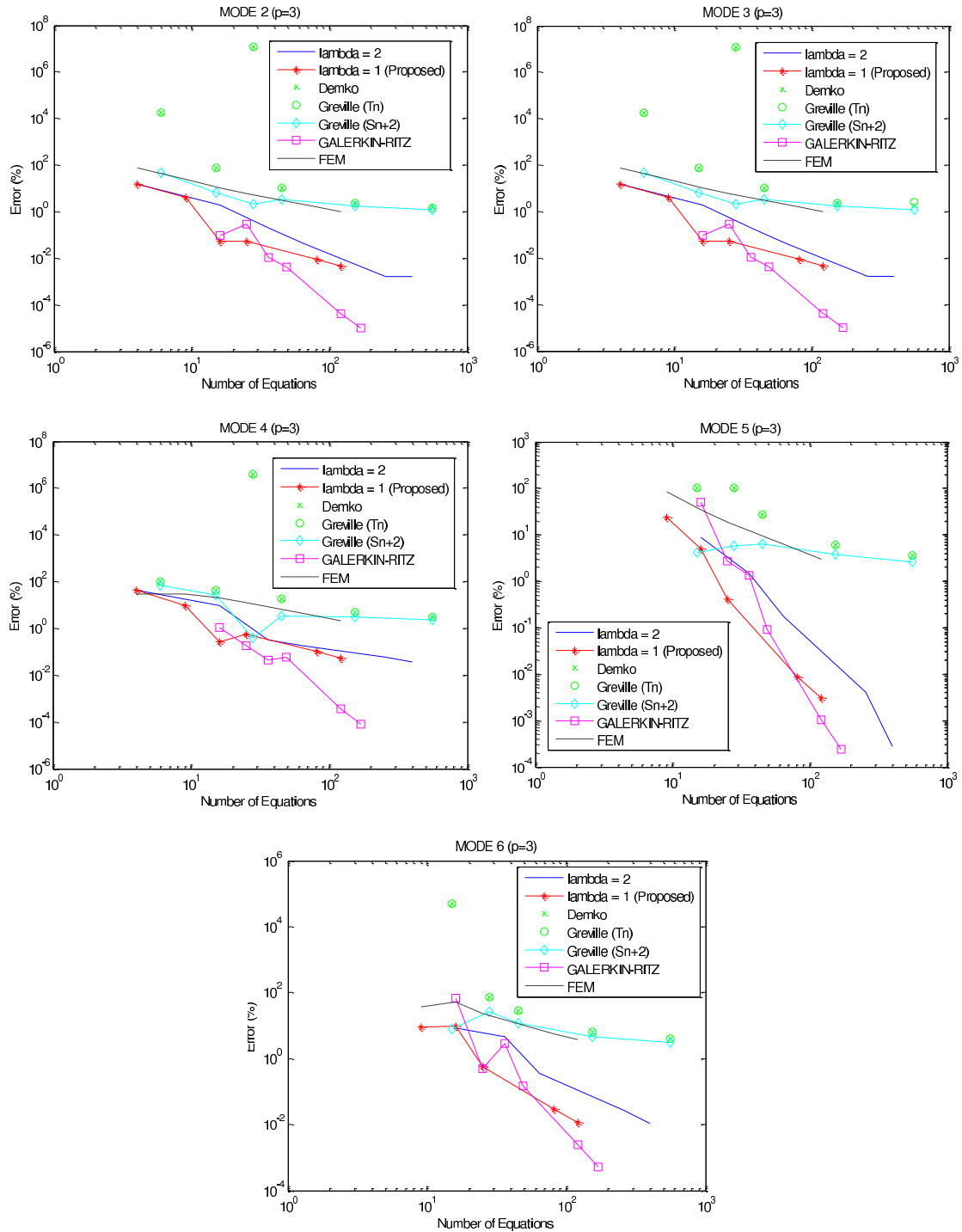


Figure 6. Circular cavity under *Neumann* boundary conditions: convergence of the first five nonzero eigenvalues in terms of number of equations, for cubic B-splines approximation ($p = 3$).

It is worth repeating that the domain integration for calculating the matrices involved in B-splines Galerkin–Ritz method was performed in conjunction with 4×4 (in general: $(p + 1) \times (p + 1)$) Gauss points per cell of breakpoints; this is four times higher than the proposed global collocation method (independently of the multiplicity of internal knots).

Concerning the elimination of the coefficients that are associated to the boundary, in the proposed global collocation method they have to be eliminated *independently* on the type of boundary conditions. In more detail, in the case of Dirichlet boundary conditions they are simply erased whereas in the Neumann case they are properly incorporated into internal ones. In contrast, in the B-splines Galerkin–Ritz formulation, only Dirichlet-type boundary conditions require the elimination of those coefficients associated to the boundary, whereas in the free-free problem the mass and stiffness matrices remain as they are.

Concerning the two examples of this study, we make some remarks:

Example 1: Rectangular cavity. No difficulty appeared in the implementation of the proposed theory for both types of boundary conditions. Concerning the particular elimination required in the Neumann problem, the standard equation (24) is generally applicable. It was found that, for both multiplicities, it is sufficient to consider only one boundary equation at each of the four corners (A, B, C, D), which is the derivative in either x - or y -direction. As previously mentioned at the end of Section 3.4.2, it is also possible to consider both directions but then it becomes necessary to apply a least-squares procedure so as to derive a square matrix \mathbf{B}_{22} ; in this case the results did not change at all. Moreover, for the particular case of a cubic polynomial ($p = 3$) and double knots ($\lambda = 2$), we can alternatively apply a more schematic procedure as shown in Appendix B.

Example 2: Circular cavity. This study reduces to cubic B-splines ($p = 3$) only. Unlike the rectangular cavity, this example requires a careful programming. First of all, the determination of the circle is not a unique procedure. In all cases we have to divide the circumference into four equal parts: AB, BC, CD and DA . Then, for a given number of n_x uniform subdivisions per side using $(n_x + 1)$ breakpoints along (e.g., AB), and for a given multiplicity ($\lambda = 1$ or 2), there are either $(n_x + 3)$ or $2(n_x + 1)$ control points, respectively, to be determined. In all cases, the extreme control points coincide with the ends of the corresponding side (e.g., AB). The internal control points were determined using boundary-only Coons interpolation.

- ▷ In the case of double knots ($\lambda = 2$), it was found reasonable at every breakpoint to consider the values of both the coordinates ($x = r \cos \phi$, $y = r \sin \phi$) and the slopes ($dx/d\phi = -r \sin \phi$, $dy/d\phi = r \cos \phi$), with $\phi = (\pi/2)\xi$, $0 \leq \xi \leq 1$.
- ▷ In the case of single knots ($\lambda = 1$), it was found sufficient to consider $n_x + 1$ uniformly arranged internal breakpoints, that is, $n_x + 2$ uniform segments.

Under these conditions, the following findings were noticed:

- For double knots ($\lambda = 2$), the derivative at the corners becomes singular due to the vanishing Jacobian determinant. In more details, at the corner “A” it holds: $(\partial x/\partial \xi = \partial x/\partial \eta = 0)$. This shortcoming was resolved considering one point before and one after the corner A (for example, in the midpoints of the adjacent control points) and then taking the mean average of the normal derivatives.
- For single knots ($\lambda = 1$), no difficulty was observed.

- When the internal control points were determined by smoothing the initial positions derived by boundary-only Coons interpolation, the accuracy of the numerical solution decreased.

In summary, for both examples of this study, the quality of the B-splines Galerkin–Ritz solution was the highest compared to that of the collocation schemes. Having said this, we must mention that the same quality of results had been previously received when using the well known tensor product Lagrange polynomials or Coons–Gordon transfinite interpolation (see [Provatidis 2006, p. 6702; Provatidis 2004, p. 49; Provatidis 2009a, pp. 486–492], among others). In other words, the high quality of the numerical solution is *due more to the global character* of any CAD-based interpolation (global approximation of the acoustic pressure) and less on the individual methodology (Galerkin–Ritz or collocation).

Although it was a study in depth, this article has some weaknesses that must be cured in our ongoing future research. One weak point is that the study does not focus on the bandwidth of the produced matrices (or better on the required CPU-time) but only on the number of equations per numerical scheme, a fact that may somehow influence the conclusions. A second point is that the second example (circular cavity) has to be studied again using NURBS in conjunction with higher polynomial degrees. A third point is that this paper refers only to cases where the basis functions have either maximum continuity (multiplicity of 1) or continuity reduced by one (multiplicity of $p - 1$) at all internal knot lines. In the future, cases where continuity is different at different knot lines should be tested.

7. Conclusions

The proposed global collocation method was based on tensor product B-splines, which are also used in the Galerkin–Ritz formulation. Unlike the latter, the estimation of mass and stiffness matrices does not need any domain integral to be computed, thus reducing the computer effort. The proposed method is applicable using either single or multiple internal knots, where the maximum allowed multiplicity equals the polynomial degree minus one. In general, multiple knots are preferred as they do not require any least-squares scheme and they lead to a rather better quality. Alternatively, isogeometric collocation should be carefully applied in conjunction with single knots, particularly in problems of Dirichlet-type boundary conditions. Obviously, the extension of the proposed approach from acoustics to elastodynamics and other types of partial differential operators as well as to three-dimensional problems is straightforward.

Appendix A: Solving boundary-value problems

The solution of the ordinary differential equation (ODE)

$$D(u(x)) = f, \quad x \in [0, L], \quad (\text{A.1})$$

by collocation is conducted as follows.

The variable is written as a B-splines series expansion

$$u(x) = \sum_{i=1}^q N_{i,p}(x) \cdot a_i, \quad (\text{A.2})$$

where q is the number of control points, $N_{i,p}$ the basis functions, and a_i the unknown coefficients. Between alternatives, it is proposed to start with a mesh of $(n + 1)$ discrete breakpoints (i.e., n segments,

uniform or not). For a given polynomial degree p , considering a given standard multiplicity λ of all inner points (see [Piegl and Tiller 1995; de Boor 2001]), we have that

$$q = p + 1 + \lambda(n - 1). \quad (\text{A.3})$$

For reasons that will be explained below, we use λ collocation points per cell, that is, between any two successive breakpoints. Then the total number of collocation points becomes

$$n_{\text{col}} = \lambda n. \quad (\text{A.4})$$

The overall computational procedure is as follows:

- (1) First the ODE is fulfilled at the above-mentioned n_{col} collocation points (this procedure is identical with that used in the eigenvalue problem), which leads to the matrix equation

$$[\mathbf{A}_{\text{col}}]_{n_{\text{col}} \times q} \cdot \begin{bmatrix} a_1 \\ \vdots \\ a_q \end{bmatrix} = \begin{bmatrix} f_1 \\ \vdots \\ f_{n_{\text{col}}} \end{bmatrix}. \quad (\text{A.5})$$

- (2) Then the boundary conditions are imposed. We distinguish two cases:

- (a) Two Dirichlet-type boundary conditions:

$$x = 0 \Rightarrow a_1 = \bar{U}_0 \quad \text{and} \quad x = L \Rightarrow a_q = \bar{U}_L. \quad (\text{A.6})$$

In this case, (A.6) are substituted into (A.5), the first (with elements a_{i1} , $i = 1, \dots, n_{\text{col}}$) and last (with elements a_{iq} , $i = 1, \dots, n_{\text{col}}$) columns of matrix $[\mathbf{A}_{\text{col}}]$ are multiplied by the known quantities \bar{U}_0 and \bar{U}_L and then these terms are transferred to the right-hand-side. In this way, the dimensions of matrix $[\mathbf{A}_{\text{col}}]$ reduce from $n_{\text{col}} \times q$ to $n_{\text{col}} \times (q - 2)$ and the equations system to be solved becomes

$$[\bar{\mathbf{A}}_{\text{col}}]_{n_{\text{col}} \times (q-2)} \cdot \begin{bmatrix} a_2 \\ \vdots \\ a_{q-1} \end{bmatrix} = \begin{bmatrix} f_1 - a_{11}\bar{U}_0 - a_{1q}\bar{U}_L \\ \vdots \\ f_{n_{\text{col}}} - a_{n_{\text{col},1}}\bar{U}_0 - a_{n_{\text{col},q}}\bar{U}_L \end{bmatrix}. \quad (\text{A.7})$$

In the sequence we shall seek for the conditions for which the aforementioned reduced matrix $[\bar{\mathbf{A}}_{\text{col}}]$ becomes *square* (with equal number of rows and columns). Actually, the combination of (A.3) and (A.4) gives

$$q - 2 = \lambda n + (p - 1 - \lambda). \quad (\text{A.8})$$

Therefore, if one selects that

$$\lambda = p - 1, \quad (\text{A.9})$$

the parenthesis in (A.8) vanishes and gives that $q - 2 = \lambda n$, which in turn, by virtue of (A.4), gives the desired relationship $n_{\text{col}} = (q - 2)$, ensuring that matrix $[\bar{\mathbf{A}}_{\text{col}}]$ is square.

- (b) One Dirichlet- and one Neumann-type boundary condition:

$$a_1 = \bar{U}_0 \quad (\text{A.10})$$

and

$$\left(\frac{\partial u}{\partial x}\right)_{x=L} = \bar{q}_L. \tag{A.11}$$

In this case, we take the first derivative of (A.2) over x and equate it with \bar{q}_L according to (A.11). Thus the number of equations is increased by one and becomes equal to $(n_{\text{col}} + 1)$ while the first column is erased (as previously), since all relevant elements are multiplied by the known value \bar{U}_0 , and is then transferred to the right hand side. Again the equations matrix is square, but in this case it is of dimensions $(n_{\text{col}} + 1) \times (n_{\text{col}} + 1)$.

Remark. Another alternative is to consider a greater number of collocation points than previously, that is $n_{\text{col}} > \lambda n$. In this case, after the boundary conditions are imposed the obtained matrix $[\bar{A}_{\text{col}}]$ is *nonsquare*, of dimensions $n_{\text{col}} \times (q - 2)$, that is with more equations than the unknowns. The remedy to obtain a numerical solution is to apply a least-squares scheme, for example multiplying both parts of (A.7) by the transpose of matrix $[\bar{A}_{\text{col}}]$. However, the time-consuming transpose-matrix concept is always solved by a QR-decomposition least-squares solver (which can be found in LINPACK, LAPACK, etc.). In this way, the solution time increment is almost negligible when compared to a regular QR-decomposition for a square matrix. Nevertheless, the built up of more rows (collocation points) than necessary is the main source of increased computer time.

Appendix B: Elimination of boundary coefficients for the free-free problem in a rectangular

We deal with the particular case in which the polynomial degree is $p = 3$ whereas the multiplicity of internal knots equals to *two* ($\lambda = 2$). In other words, we consider *double* knots.

Let us consider a rectangle $ABCD$ as shown in Figure 7. The opposite sides AB and CD are divided into n_x uniform subdivisions, whereas the other opposite sides (BC and DA) are divided into n_y uniform ones. The axis origin is taken at the corner A .

In case of piecewise cubic polynomials ($p = 3$) the first control point P_0 coincides with the corner A , whereas P_{2n_x+1} coincides with the corner B . The second layer consists of the control points ($P_{2(n_x+1)}$ up to $P_{4(n_x+1)-1}$), and so on. Obviously, the last control point is $P_{4(n_x+1) \times (n_y+1) - 1}$, and it coincides with

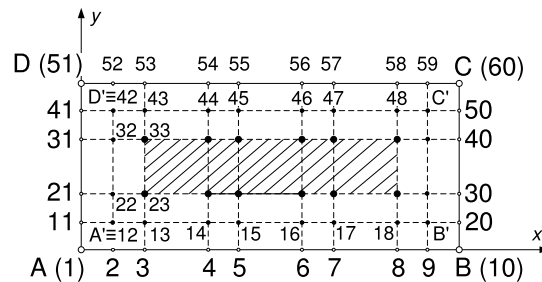


Figure 7. A sketch, for $n_x \times n_y = 4 \times 2$ subdivisions and double knots ($\lambda = 2$) for cubic B-splines ($p = 3$), aiming at describing the procedure of eliminating the coefficients associated to the boundary control points in a rectangular $ABCD$. The hatched area indicates those internal control points that are not influenced by the aforementioned elimination.

the upper right corner C (Figure 7). Henceforth, for the sake of simplicity we limit the discussion for the particular case of $n_x \times n_y = 4 \times 2$ subdivisions, where we change the numbering of the control points, starting from “1” (corner A) and ending at “60” (corner C).

Taking the first derivative of (13) with respect to the unit normal vector \mathbf{n} (at a point along the side DA), we obtain

$$\left. \frac{\partial u}{\partial \mathbf{n}} \right|_{DA} = \sum_{k=1}^q \frac{\partial \phi_k(0, \eta)}{\partial \mathbf{n}} \cdot a_k, \quad (\text{B.1})$$

where, as already explained, it holds that

$$q = 4(n_x + 1) \times (n_y + 1). \quad (\text{B.2})$$

First, (B.1) is applied at the control point $\mathbf{P}_0 \equiv A$, and due to the free-free boundary conditions we obtain

$$\sum_{k=1}^q \frac{\partial \phi_k(0, 0)}{\partial x} \cdot a_k = 0. \quad (\text{B.3})$$

Due to the compact support of the basis functions $N_{i,p}(\xi)$ and $N_{j,p}(\eta)$, (B.3) is written as

$$\sum_{l=1}^{2(n_x+1)} b_{lx} \cdot a_l = 0, \quad (\text{B.4})$$

with

$$b_{lx} = \frac{\partial \phi_l}{\partial x}(0, 0), \quad l = 1, \dots, 2(n_x + 1). \quad (\text{B.5})$$

Applying (B.3) at all control points along the boundary, we can obtain several relationships:

$$\text{between “1” and “2”}: b_{1x}a_1 + b_{2x}a_2 = 0. \quad (\text{B.6})$$

Equation (B.6) induces a linear relationship between the coefficients a_1 and a_2 associated to control points “1” and “2”, respectively.

Moreover, we can write one identical relationship between the control points “11” and “12”:

$$\text{between “11” and “12”}: b_{1x}a_{11} + b_{2x}a_{12} = 0 \Rightarrow a_{11} = -\frac{b_{2x}}{b_{1x}}a_{12}. \quad (\text{B.7})$$

In an analogous way, taking the derivatives in the y -direction, we can write:

$$\text{between “1” and “11”}: b_{1y}a_1 + b_{2y}a_{11} = 0, \quad (\text{B.8})$$

$$\text{between “2” and “12”}: b_{1y}a_2 + b_{2y}a_{12} = 0 \Rightarrow a_2 = -\frac{b_{2y}}{b_{1y}}a_{12}. \quad (\text{B.9})$$

Equations (B.6)–(B.9) impose four equations for the four variables: a_1 , a_2 , a_{11} (to be eliminated) and the a_{12} (to be kept). Therefore, it is anticipated that one of them is redundant. In fact, substituting (B.6), which is related to the derivative in the x -direction, into (B.9) one obtains the relationship between the corner “1” and the close-to-corner “12” control point as

$$a_1 = \frac{b_{2x}}{b_{1x}} \cdot \frac{b_{2y}}{b_{1y}} \cdot a_{12}. \quad (\text{B.10})$$

Obviously, the same relationship is also derived starting from the derivative at the corner “1” in the y -direction, that is, substituting (B.8) into (B.7):

$$a_1 = -\frac{b_{2y}}{b_{1y}}a_{11} = -\frac{b_{2y}}{b_{1y}} \cdot \left(-\frac{b_{2x}}{b_{1x}} \cdot a_{12}\right) = \frac{b_{2y}}{b_{1y}} \cdot \frac{b_{2x}}{b_{1x}} \cdot a_{12}. \tag{B.11}$$

The above fact (identity between (B.10) and (B.11)) depicts that it is *not* necessary to consider *both* fluxes at the corner. Therefore, we can ignore, for example, (B.8) and derive unique expression between points 11 and 12 (B.7), as well as between “2” and “12” (B.9). Moreover, the relationship between the control points “3” with “13” is similar to that between “2” and “12”. Generally, all intermediate control points along AB are slaves of the master points along the internal boundary $A'B'$ (Figure 7). In an analogous way, we can obtain master-to-slave relations for the control points along the remaining sides AB , BC , and CD . In this way, all control points along the boundary are slaves and are substituted by the master control points along the line $A'B'C'D'$ shown in Figure 7.

In order to analytically perform the elimination, let us now consider an arbitrary collocation point “ i ” (not shown in Figure 7). The i -th row of the matrix equation is written as

$$\begin{aligned} &(m_{i,1}\ddot{a}_1 + m_{i,2}\ddot{a}_2 + \dots + m_{i,11}\ddot{a}_{11} + m_{i,12}\ddot{a}_{12} + \dots + m_{i,60}\ddot{a}_{60}) \\ &\quad + (k_{i,1}a_1 + k_{i,2}a_2 + \dots + k_{i,11}a_{11} + k_{i,12}a_{12} + \dots + k_{i,60}a_{60}) = 0. \end{aligned} \tag{B.12}$$

In (B.12) we substitute the boundary values such as a_1 using (B.10), a_2 using (B.9), a_{11} using (B.7) and so on. In this way, the coefficient a_{12} appears as a factor of four terms, the coefficients a_{13} to a_{18} appear as factors of two terms, the coefficient a_{19} appears as a factor again of four terms, and so on. In more detail, after the above-mentioned substitutions equation (B.12) is written as

$$\begin{aligned} \ddot{a}_{12} &\left[m_{i,1} \left(\frac{b_{2y}}{b_{1y}} \cdot \frac{b_{2x}}{b_{1x}} \right) + m_{i,2} \left(-\frac{b_{2y}}{b_{1y}} \right) + m_{i,11} \left(-\frac{b_{2x}}{b_{1x}} \right) + m_{i,12} \right] \\ &\quad + \ddot{a}_{13} \left[\left(-\frac{b_{2y}}{b_{1y}} \right) m_{i,3} + m_{i,13} \right] + \dots + \ddot{a}_{18} \left[\left(-\frac{b_{2y}}{b_{1y}} \right) m_{i,8} + m_{i,18} \right] + \dots \\ &\quad + a_{12} \left[k_{i,1} \left(\frac{b_{2y}}{b_{1y}} \cdot \frac{b_{2x}}{b_{1x}} \right) + k_{i,2} \left(-\frac{b_{2y}}{b_{1y}} \right) + k_{i,11} \left(-\frac{b_{2x}}{b_{1x}} \right) + k_{i,12} \right] \\ &\quad + a_{13} \left[\left(-\frac{b_{2y}}{b_{1y}} \right) k_{i,3} + k_{i,13} \right] + \dots + a_{18} \left[\left(-\frac{b_{2y}}{b_{1y}} \right) k_{i,8} + k_{i,18} \right] + \dots = 0. \end{aligned} \tag{B.13}$$

Obviously, the implementation of (B.13) and its analogue reduces the order of each matrix from $4(n_x + 1)(n_y + 1)$ to $4(n_x - 1)(n_y - 1)$.

In summary, those control points deeply in the interior (large black circles) are not influenced by the Neumann conditions and keep their columns. The remaining internal control points (small black circles) that are in the first layer parallel to the boundary are divided into two categories. The first category consists of only the four control points A' , B' , C' , and D' that lie in the neighborhood of the four corners; the corresponding condensed matrix elements are composed of *four* values (cf. a_{12} in (B.13)). The second category consists of those intermediate control points along the internal boundary $A'B'C'D'$ (Figure 7); the corresponding condensed matrix elements are composed of *two* values (cf. a_{13} in (B.13)).

References

- [Auricchio et al. 2010] F. Auricchio, L. Beirão da Veiga, T. J. R. Hughes, A. Reali, and G. Sangalli, “Isogeometric collocation methods”, *Math. Models Methods Appl. Sci.* **20**:11 (2010), 2075–2107.
- [Bézier 1971] P. E. Bézier, “Example of an existing system in the motor industry: the Unisurf system”, *Proc. R. Soc. Lond. A* **321**:1545 (1971), 207–218.
- [Bialecki et al. 2011] B. Bialecki, G. Fairweather, and A. Karageorghis, “Matrix decomposition algorithms for elliptic boundary value problems: a survey”, *Numer. Algorithms* **56**:2 (2011), 253–295.
- [de Boor 1972] C. de Boor, “On calculating with *B*-splines”, *J. Approx. Theory* **6** (1972), 50–62.
- [de Boor 2001] C. de Boor, *A practical guide to splines*, Revised ed., Applied Mathematical Sciences **27**, Springer, New York, 2001.
- [Cabral et al. 1990] J. J. S. P. Cabral, L. C. Wrobel, and C. A. Brebbia, “A BEM formulation using *B*-splines, I: Uniform blending functions”, *Eng. Anal. Bound. Elem.* **7**:3 (1990), 136–144.
- [Cabral et al. 1991] J. J. S. P. Cabral, L. C. Wrobel, and C. A. Brebbia, “A BEM formulation using *B*-splines, II: Multiple knots and non-uniform blending functions”, *Eng. Anal. Bound. Elem.* **8**:1 (1991), 51–55.
- [Coons 1967] S. A. Coons, “Surfaces for computer-aided design of space forms”, Technical Report MIT/LCS/TR-41, Massachusetts Institute of Technology, Cambridge, MA, June 1967, Available at <http://publications.csail.mit.edu/lcs/pubs/pdf/MIT-LCS-TR-041.pdf>.
- [Cottrell et al. 2009] J. A. Cottrell, T. J. R. Hughes, and Y. Bazilevs, *Isogeometric analysis: toward integration of CAD and FEA*, Wiley, Chichester, 2009.
- [Fairweather and Meade 1989] G. Fairweather and D. Meade, “A survey of spline collocation methods for the numerical solution of differential equations”, pp. 297–341 in *Mathematics for large scale computing*, edited by J. C. Díaz, Lecture Notes in Pure and Appl. Math. **120**, Dekker, New York, 1989.
- [Farin et al. 2002] G. Farin, J. Hoschek, and M.-S. Kim (editors), *Handbook of computer aided geometric design*, North-Holland, Amsterdam, 2002.
- [Filippatos 2010] A. Filippatos, *Derivation of eigenfrequencies in acoustic cavities and elastic structures using the global collocation method*, thesis, National Technical University of Athens, October 2010.
- [Gordon 1971] W. J. Gordon, “Blending-function methods of bivariate and multivariate interpolation and approximation”, *SIAM J. Numer. Anal.* **8** (1971), 158–177.
- [Höllig 2003] K. Höllig, *Finite element methods with *B*-splines*, Frontiers in Applied Mathematics **26**, Society for Industrial and Applied Mathematics, Philadelphia, 2003.
- [Hughes et al. 2010] T. J. R. Hughes, A. Reali, and G. Sangalli, “Efficient quadrature for NURBS-based isogeometric analysis”, *Comput. Methods Appl. Mech. Eng.* **199**:5-8 (2010), 301–313.
- [Jerome and Varga 1969] J. W. Jerome and R. S. Varga, “Generalizations of spline functions and applications to nonlinear boundary value and eigenvalue problems”, pp. 103–155 in *Theory and applications of spline functions* (Madison, WI, 1968), edited by T. N. E. Greville, Academic Press, New York, 1969.
- [Kwok et al. 2001] W. Y. Kwok, R. D. Moser, and J. Jiménez, “A critical evaluation of the resolution properties of *B*-spline and compact finite difference methods”, *J. Comput. Phys.* **174**:2 (2001), 510–551.
- [Piegl 1991] L. Piegl, “On NURBS: a survey”, *IEEE Comput. Graph. Appl.* **11**:1 (1991), 55–71.
- [Piegl and Tiller 1995] L. Piegl and W. Tiller, *The NURBS Book*, Springer, London, 1995.
- [Provatidis 2004] C. G. Provatidis, “On DR/BEM for eigenvalue analysis of 2-D acoustics”, *Comput. Mech.* **35**:1 (2004), 41–53.
- [Provatidis 2006] C. G. Provatidis, “Transient elastodynamic analysis of two-dimensional structures using Coons-patch macroelements”, *Int. J. Solids Struct.* **43**:22–23 (2006), 6688–6706.
- [Provatidis 2008a] C. G. Provatidis, “Free vibration analysis of elastic rods using global collocation”, *Arch. Appl. Mech.* **78**:4 (2008), 241–250.

- [Provatidis 2008b] C. G. Provatidis, “A global collocation method for two-dimensional rectangular domains”, *J. Mech. Mater. Struct.* **3**:1 (2008), 185–193.
- [Provatidis 2008c] C. G. Provatidis, “Time- and frequency-domain analysis using lumped mass global collocation”, *Arch. Appl. Mech.* **78**:11 (2008), 909–920.
- [Provatidis 2009a] C. G. Provatidis, “Eigenanalysis of two-dimensional acoustic cavities using transfinite interpolation”, *J. Algorithms Comput. Technol.* **3**:4 (2009), 477–502.
- [Provatidis 2009b] C. G. Provatidis, “Integration-free Coons macroelements for the solution of 2D Poisson problems”, *Int. J. Numer. Methods Eng.* **77**:4 (2009), 536–557.
- [Provatidis 2012] C. G. Provatidis, “Two-dimensional elastostatic analysis using Coons–Gordon interpolation”, *Meccanica (Milano)* **47**:4 (2012), 951–967.
- [Provatidis and Ioannou 2010] C. G. Provatidis and K. S. Ioannou, “Static analysis of two-dimensional elastic structures using global collocation”, *Arch. Appl. Mech.* **80**:4 (2010), 389–400.
- [Schoenberg 1946] I. J. Schoenberg, “Contributions to the problem of approximation of equidistant data by analytic functions, A: On the problem of smoothing or graduation. A first class of analytic approximation formulae”, *Quart. Appl. Math.* **4** (1946), 45–99. Available in *I. J. Schoenberg: selected papers*, Vol. 2, pp. 3–57, edited by C. de Boor, Birkhäuser, Boston, 1988.
- [Schoenberg and Whitney 1953] I. J. Schoenberg and A. Whitney, “On Pólya frequency functions, III: The positivity of translation determinants with an application to the interpolation problem by spline curves”, *Trans. Amer. Math. Soc.* **74** (1953), 246–259.

Received 19 Oct 2011. Revised 10 Mar 2014. Accepted 21 Mar 2014.

CHRISTOPHER G. PROVATIDIS: cprovat@central.ntua.gr

School of Mechanical Engineering, Mechanical Design and Control Systems Department, National Technical University of Athens, Heron Polytechniou 9, Zografou Campus, 157 80 Athens, Greece

JOURNAL OF MECHANICS OF MATERIALS AND STRUCTURES

msp.org/jomms

Founded by Charles R. Steele and Marie-Louise Steele

EDITORIAL BOARD

ADAIR R. AGUIAR	University of São Paulo at São Carlos, Brazil
KATIA BERTOLDI	Harvard University, USA
DAVIDE BIGONI	University of Trento, Italy
IWONA JASIUK	University of Illinois at Urbana-Champaign, USA
THOMAS J. PENCE	Michigan State University, USA
YASUhide SHINDO	Tohoku University, Japan
DAVID STEIGMANN	University of California at Berkeley

ADVISORY BOARD

J. P. CARTER	University of Sydney, Australia
D. H. HODGES	Georgia Institute of Technology, USA
J. HUTCHINSON	Harvard University, USA
D. PAMPLONA	Universidade Católica do Rio de Janeiro, Brazil
M. B. RUBIN	Technion, Haifa, Israel

PRODUCTION production@msp.org

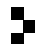
SILVIO LEVY Scientific Editor

See msp.org/jomms for submission guidelines.

JoMMS (ISSN 1559-3959) at Mathematical Sciences Publishers, 798 Evans Hall #6840, c/o University of California, Berkeley, CA 94720-3840, is published in 10 issues a year. The subscription price for 2014 is US\$555/year for the electronic version, and \$710/year (+\$60, if shipping outside the US) for print and electronic. Subscriptions, requests for back issues, and changes of address should be sent to MSP.

JoMMS peer-review and production is managed by EditFLOW[®] from Mathematical Sciences Publishers.

PUBLISHED BY

 **mathematical sciences publishers**
nonprofit scientific publishing

<http://msp.org/>

© 2014 Mathematical Sciences Publishers

Journal of Mechanics of Materials and Structures

Volume 9, No. 3

May 2014

- B-splines collocation eigenanalysis of 2D acoustic problems**
CHRISTOPHER G. PROVATIDIS 259
- Multi-region Trefftz collocation grains (MTCGs) for modeling piezoelectric composite and porous materials in direct and inverse problems**
PETER L. BISHAY, ABDULLAH ALOTAIBI and SATYA N. ATLURI 287
- Analytical solution for ductile and FRC plates on elastic ground loaded on a small circular area**
ENRICO RADI and PIETRO DI MAIDA 313
- Solution of a receding contact problem using an analytical method and a finite element method**
ERDAL ÖNER, MURAT YAYLACI and AHMET BIRINCI 333
- Sliding of a cup-shaped die on a half-space: influence of thermal relaxation, convection and die temperature**
LOUIS MILTON BROCK 347



1559-3959(2014)9:3;1-7